MTOpen

Optogenetic Vision Restoration Using Rhodopsin for Enhanced Sensitivity

Benjamin M Gaub[1], Michael H Berry[2], Amy E Holt[2], Ehud Y Isacoff[1–3] and John G Flannery[1,2,4]

[1]Helen Wills Neuroscience Institute, University of California Berkeley, Berkeley, California, USA; [2]Department of Molecular and Cell Biology, University of California Berkeley, Berkeley, California, USA; [3]Physical Bioscience Division, Lawrence Berkeley National Laboratory, Berkeley, California, USA; [4]Vision Science, University of California, Berkeley, California, USA.

Retinal disease is one of the most active areas of gene therapy, with clinical trials ongoing in the United States for five diseases. There are currently no treatments for patients with late-stage disease in which photoreceptors have been lost. Optogenetic gene therapies are in development, but, to date, have suffered from the low light sensitivity of microbial opsins, such as channelrhodopsin and halorhodopsin, and azobenzene-based photoswitches. Several groups have shown that photoreceptive G-protein-coupled receptors (GPCRs) can be expressed heterologously, and photoactivate endogenous $G_{i/o}$ signaling. We hypothesized such a GPCR could increase sensitivity due to endogenous signal amplification. We targeted vertebrate rhodopsin to retinal ON-bipolar cells of blind *rd1* mice and observed restoration of: (i) light responses in retinal explants, (ii) visually-evoked potentials in visual cortex *in vivo*, and (iii) two forms of visually-guided behavior: innate light avoidance and discrimination of temporal light patterns in the context of fear conditioning. Importantly, both the light responses of the retinal explants and the visually-guided behavior occurred reliably at light levels that were two to three orders of magnitude dimmer than required for channelrhodopsin. Thus, gene therapy with native light-gated GPCRs presents a novel approach to impart light sensitivity for visual restoration in a useful range of illumination.

Received 28 January 2015; accepted 22 June 2015; advance online publication 28 July 2015. doi:10.1038/mt.2015.121

INTRODUCTION

Most forms of inherited blindness result from photoreceptor cell death caused by mutations in photoreceptor cell-specific genes. In many of these conditions, the second and third order retinal interneurons remain electrically active,[1–4] even after the retina has lost sensitivity to light due to loss of the photoreceptors, providing an opportunity for treatment. Tremendous progress has been made toward gene replacement therapy for certain retinal diseases.[5–7] Current gene therapy technology requires a specific vector for each gene defect, making clinical treatment very costly and creating a need for mutation independent approaches. One approach for late-stage retinal degeneration has recently been approved for human use and functions irrespective of the genetic cause of vision loss. It is based on electrical stimulation of the surviving neurons in the retina via implanted electrode arrays that receive input from a camera.[8,9] Spatial information about the surrounding environment is converted to electrical impulses, which in turn excite retinal neurons in proximity of the electrode. This has been shown to restore light sensitivity and low acuity vision to blind patients, but is costly, and current designs offer low resolution. Other proposed therapies impart light sensitivity to the surviving retinal interneurons using genetically-encoded light-gated proteins,[10–16] photosensitive chemicals[17,18] or a combination of the two.[19–21] The microbial light-sensitive proteins channelrhodopsin (ChR2) and halorhodopsin (NpHr) have been targeted to cone photoreceptors that have lost their outer segments,[11] ON-bipolar cells (ON-BCs)[12,14–16] and retinal ganglion cells (RGCs),[10] leading to successful restoration of basic visual functions in mouse models of blindness. Microbial opsins are relatively simple to work with and have important benefits—following the gene transfer to the target cell, the apo-protein is stably expressed[14] and the cell remains light sensitive without further additions due to bioavailability of the required chromophore 11-cis-retinal. In contrast, optochemical treatment utilizes synthetic azobenzene-based photoswitches designed to activate endogenous receptors[17,18] or engineered mammalian receptors and channels.[19–21] These synthetic photoswitches have a limited half-life and need to be resupplied on a regular basis. All of these optogenetic and optochemical tools provide inadequate light sensitivity to function in normal daylight and avoid damage to residual photoreceptors by hardware-dependent intensification.

The operation of the optogenetic ion channels and pumps differs substantially from the rod and cone opsin GPCRs of wild-type photoreceptors. Only the GPCRs have integral signal amplification cascades in which a single photon can activate multiple G-proteins, leading to hydrolysis of hundreds to thousands of cGMP molecules that gate downstream cyclic nucleotide-gated channels.[22] Attempting to increase light sensitivity by increasing the expression of the optogenetic sensor protein is problematic because of increased risk for cell toxicity[23] and immune response.[23,24] An elegant approach to circumvent these issues has

Correspondence: John G Flannery, Helen Wills Neuroscience Institute, University of California Berkeley, Berkeley, California, USA.
E-mail: flannery@berkeley.edu or Ehud Y Isacoff, Helen Wills Neuroscience Institute, University of California Berkeley, Berkeley, California, USA.
E-mail: ehud@berkeley.edu

been to use the native light-gated GPCR melanopsin from intrinsically photosensitive RGCs.[13] When targeted to all RGCs of *rd1* mice, melanopsin rescued retinal light responses and enabled innate and learned behavior at very dim light conditions.[13] Unfortunately, the slow (seconds) kinetics of melanopsin exclude it from practical use for vision of moving objects and visually-guided motility.

Here, we used another native opsin GPCR: rhodopsin. We expressed rhodopsin in ON-BCs, second-order neurons, which receive synaptic input from photoreceptor cells. We chose to target ON-BCs[25,26] because they are located upstream in the retinal circuitry, do not exhibit significant remodeling until late stages of degeneration and because their normal mode of activation is by glutamate released from photoreceptors that acts on a GPCR, the metabotropic glutamate receptor mGluR6.[27] Vertebrate rhodopsin delivered to ON-BCs by an adeno-associated virus (AAV) viral vector restored light responses to blind *rd1* mouse retinas, at light levels 2–3 orders of magnitude lower than required for ChR2 in ON-BCs. Enhanced light sensitivity was also seen *in vivo* in visually-evoked potentials (VEPs) recorded in primary visual cortex and in two visually-guided behaviors: an innate photo-phobic behavior, and a simple associative learning to discriminate moving from static stimuli. Taken together, we show that gene therapy with light-gated GPCRs presents a promising approach to developing a retinal prosthetic with increased sensitivity while avoiding complications associated with immunoreactivity.

RESULTS

Rhodopsin can be expressed ectopically in ON-bipolar cells of the *rd1* mouse retina

We tested the functionality of rhodopsin for vision restoration in the *rd1* mouse in which retinal degeneration is caused by a mutation in the PDE-6-β gene, resulting in rapid loss of rod photoreceptors, followed by progressive loss of cones, leading to blindness by postnatal day 90.[28] We used an AAV viral vector and a cell-specific promoter to drive expression of the rhodopsin protein in ON-BCs of the *rd1* mouse retina *in vivo*. Several groups have demonstrated successful targeting of ON-BCs in the mouse retina using a combination of different viral vectors and promoters.[14–16,21] ON-BCs are located in the middle layer of the retina between the RGC layer and the photoreceptor cell layer (**Figure 1a**), making these cells difficult to access with viral vectors from either side of the retina. Modified virus variants have been developed with increased retinal penetration to access inner retinal neurons. Two recent studies used directed evolution to select for AAV variants with enhanced expression in photoreceptor cells[29] or ON-BCs[15,16] when injected in the vitreous. We chose a different strategy utilizing the quadruple tyrosine mutant AAV2/2(4YF) variant,[30] which is protected from proteasome degradation, and thus leads to enhanced transduction of cells in the inner retina when injected intravitreally. We restricted expression to ON-BCs, using a cell-specific promoter construct 4xgrm6,[15] based on the mouse (mGluR6) promoter.

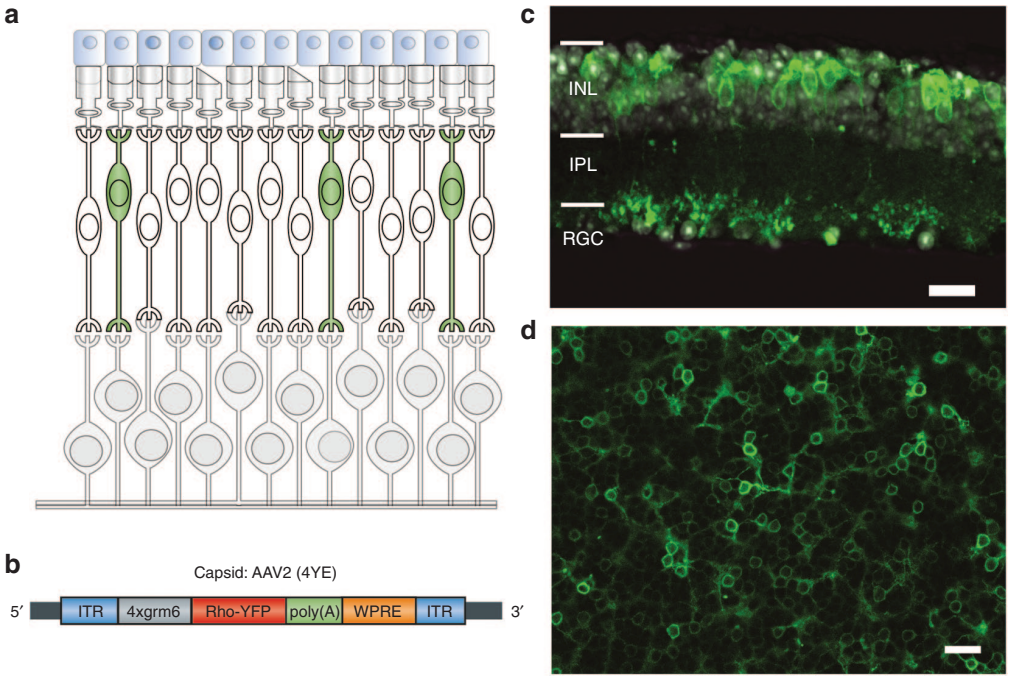

Figure 1 Rhodopsin can be expressed ectopically in ON-bipolar cells of the *rd1* mouse retina. (**a**) Schematic of a degenerated *rd1* mouse retina with target cells (ON-BC) highlighted in green. INL, inner nuclear layer; IPL, inner plexiform layer with indication of on and off sublayers; ONL, outer nuclear layer; OPL, outer plexiform layer; RGC, retinal gangion cell layer. (**b**) DNA expression cassette for the gene therapy vector. Rhodopsin is tagged (C-terminally) with yellow flourescent protein (YFP) and expression is driven by the metabotropic glutamate receptor 6 (4xgrm6) promoter. Promoter and rhodopsin-YFP sequences are flanked by inverted terminal repeat domains and stabilized by a polyadenylation signal sequence (polyA) and a woodchuck hepatitis post-transcriptional regulatory element (WPRE). The cassette was packaged into the AAV2/2 (4YF) serotype. (**c,d**) Confocal images of section (**c**) or wholemount (**d**) showing rhodopsin-YFP expression in ON-BCs of 3-month-old *rd1* mouse retina >6 weeks after intravitreal injection of AAV2/2(4YF)-4xgrm6-Rho-YFP (2 µl volume equal to 5×10^{11} viral genomes). Nuclei are stained with DAPI and pseudo colored in white. Scale bar =20 µm.

To track rhodopsin expression, we added a yellow fluorescent protein tag to the C-terminal end of the rhodopsin protein.[31] The gene expression cassette 4xgrm6-Rho-YFP (**Figure 1b**) was packaged into AAV2/2(4YF) and a volume of 2 µl (10^{10}–10^{11} viral particles) was injected intravitreally into retinas of 3–6-week-old *rd1* mice. Expression was confirmed >6 weeks after injection by imaging retinal sections (**Figure 1c**) and flat-mounted retinas (**Figure 1d**). Agarose sections confirmed ON-BC-specific expression, with fluorescently labeled processes terminating in the ON-sublayer of the inner plexiform layer (**Supplementary Figure S1a**). Stainings with rod bipolar cell marker PKC-α showed high levels of colocalization with virally expressed rhodopsin-YFP in sections (**Supplementary Figure S1b–d**) and flat-mounts (**Supplementary Figure S2**). Rhodopsin expression was strong and pan-retinal (**Supplementary Figure S1e**) and showed little cell-to-cell and retina-to-retina variability. Comparison with retinas from transgenic grm6-EGFP mice (**Supplementary Figure S1f,g**) expressing EGFP in all ON-bipolar cells revealed little difference apart from density of expression. For subsequent control experiments, we used the same promoter and vector combination (**Supplementary Figure S3a**) to target expression of the humanized enhanced (H134R) version of ChR2 to ON-BCs (**Supplementary Figure S3**). Similarly, ChR2 expression was strong and pan-retinal (**Supplementary Figure S3b,c,g**), and colocalized well with PKC-α (**Supplementary Figures S3d–f and S4**).

Rhodopsin expression in ON-BCs restores light responses to retinal explants *in vitro*

Strong rhodopsin expression in retinal ON-BCs prompted us to examine whether functional light responses were restored in retinal explants. We used a multi electrode array (MEA) to record the electrical activity of RGCs. Retinal explants from *rd1* mice (>3 months of age, n = 4 mice total), which had been injected with AAV2(4YF) 4xgrm6-Rho-YFP *in vivo* 6–8 weeks earlier, were repeatedly stimulated with full field flashes of green light (13.0 mW/cm², 510/50 nm, 10 seconds light on, 60 seconds light off). We observed robust light-evoked spiking activity in rhodopsin-treated retinas (**Figure 2b**), whereas untreated, age-matched control *rd1* retinas did not respond to the light stimulation (**Figure 2a**). The recordings were performed without supply of exogenous 11-cis-retinal. To confirm that the light responses observed in treated mice were driven by expressed rhodopsin and not by intrinsic melanopsin, we added the glutamate receptor antagonist DNQX to the bath with the rationale that cell autonomous signaling in melanopsin-expressing intrinsically photosensitive RGCs would remain unperturbed, whereas signal transmission from ON-BCs to

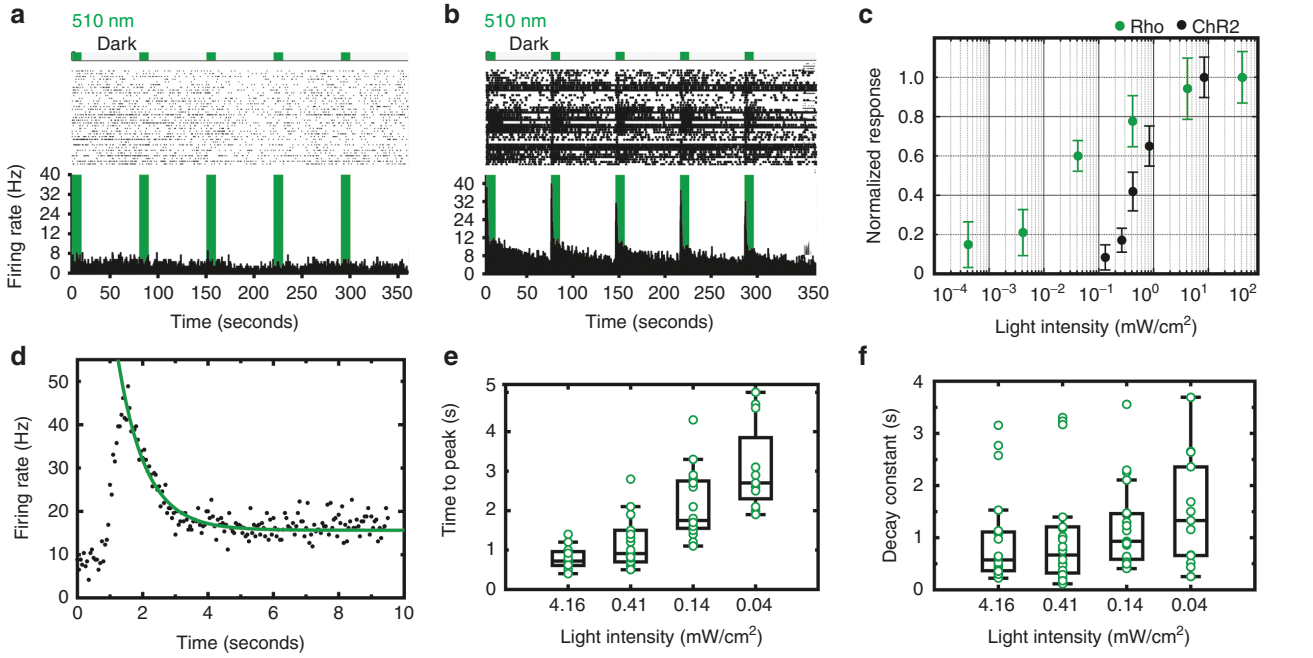

Figure 2 Rhodopsin expression in ON-BC restores light responses to retinal explants *in vitro*. (**a–f**) Data obtained by multi electrode array recordings of retinal explants from *rd1* mice. (**a**,**b**) Representative rasterplots of *rd1* mice without (**a**) or with (**b**) expression of rhodopsin in ON-BCs. Top: light stimulation protocol 5×10 seconds green light at 510/50 nm and 60 seconds dark. Middle: raster plot with spikes for all light sensitive RGCs (A: n = 36 cells, B: n = 53 cells), Bottom: peri-stimulus time histogram with 250 ms bins. (**c**) Light sensitivity for ON-BC rhodopsin *rd1* (green circles) and ON-BC ChR2 *rd1* (black circles) at 10 seconds stimulation (rhodopsin n = 20 cells, stimulated with 510/50 nm; ChR2 n = 27 cells, stimulated with 472/30 nm). Only the cells that responded to all six light steps were included in the plot. Firing rates are normalized and values are shown as means ± SEM. Light intensities on x-axis are given in mW/cm². (**d**) Kinetics for ON-BC rhodopsin *rd1*. The population averaged response (n = 53 cells) from 10 seconds stimulation was plotted as a histogram (black circles) and the signal decay was exponentially fit (green). The time constant for the population peak response decay was 0.85 seconds. Time from light flash to peak was 550 ms. (**e**,**f**) Response kinetics for ON-BC rhodopsin *rd1* (n = 20 cells) at 10 seconds stimulation with varying stimulating light intensities given as mW/cm². Only the cells that responded to all four light steps were included in the plot. (**e**) Time from flash to peak response and (**f**) peak response decay constants are shown as combined boxplot (in black showing mean, first and third quartile) and scatterplot (green open circles).

RGCs would be blocked. We found that DNQX caused loss of all fast light responses (**Supplementary Figure S5a,b**), indicating that the light responses originated upstream of the RGC layer and were independent of melanopsin. Rhodopsin elicited light responses in >50% of the electrodes of the MEA, with peak firing rates of approximately 40 Hz (**Figure 2b**). The average firing rate in the light was similar for rhodopsin treated *rd1* retinas and wild-type retinas (**Supplementary Figure S5c**). While the majority of RGCs (85%) showed an increase in firing rate upon exposure to a full-field flash of light, consistent with an ON-response, a small fraction of RGCs (7%) showed a decrease in firing rate and had a negative photoswitching index (firing rate light—firing rate dark/firing rate light + firing rate dark), consistent with OFF responses found in other recent studies in which light sensitivity was restored with ChR2 expressed in ON-BCs[15,16] (**Supplementary Figure S5d**). Addition of the metabotropic glutamate receptor 6 agonist LAP-4 had no effect on rhodopsin-induced light responses (**Supplementary Figure S5e**) proving that residual photoreceptors did not contribute to the observed signal.

Since rhodopsin is a GPCR, we hypothesized that signal amplification may enhance light sensitivity of treated retinas compared to a light-gated ion channel. We stimulated rhodopsin-treated retinas with green light (510/50 nm) at a range of different light intensities and found that rhodopsin was responsive over a wide range of intensities, spanning 5 log units from 4.2×10^{-4} to 41.6 mW/cm^2 (**Figure 2c**). Robust light responses were obtained at the lowest light intensity tested (4.2×10^{-4} mW/cm^2). By contrast, ChR2 expressed in the ON-BCs of *rd1* mice under the same conditions (same promoter, capsid, titer of virus, mode of injection, and time of expression), but stimulated with blue light (473/30 nm) to match the absorption spectrum and maximize light responses, showed a narrow intensity-response relationship, spanning only 2 log units. The minimal light intensity requirement to elicit a response was 0.1 mW/cm^2 (**Figure 2c**). The half-activation of rhodopsin-mediated signals occurred at ~200-fold lower light levels than for ChR2, a large improvement in sensitivity. We plotted the percent of cells responding to each step of light intensity (**Supplementary Figure S5f**) and found that ChR2 had a steeper drop-off compared to rhodopsin. Extrapolation of the data for lower light intensities would predict the true threshold for rhodopsin to be much lower than indicated by **Figure 2c**. The ChR2 threshold, however, should be close to the lowest light intensity tested. We recorded responses to a number of selected wavelengths using band pass filters (**Supplementary Figure S5g**). The response profile we recorded from our rhodopsin treated retinas matched well with the published spectral sensitivity curve for rhodopsin in photoreceptors.[32] Next, we quantified the kinetics of rhodopsin-mediated signals. Fits of a single exponential function to the averaged response to a single flash of light (13.0 mW/cm^2, 510/50 nm, 10 seconds) of all of the responding cells (n = 53 cells) in a single retinal region showed that the response decayed with a time-constant of 0.83 seconds (**Figure 2d,f**). Both the time to peak and the decay of the response were slower at lower intensities of the light flash (**Figure 2e,f**; n = 20 cells).

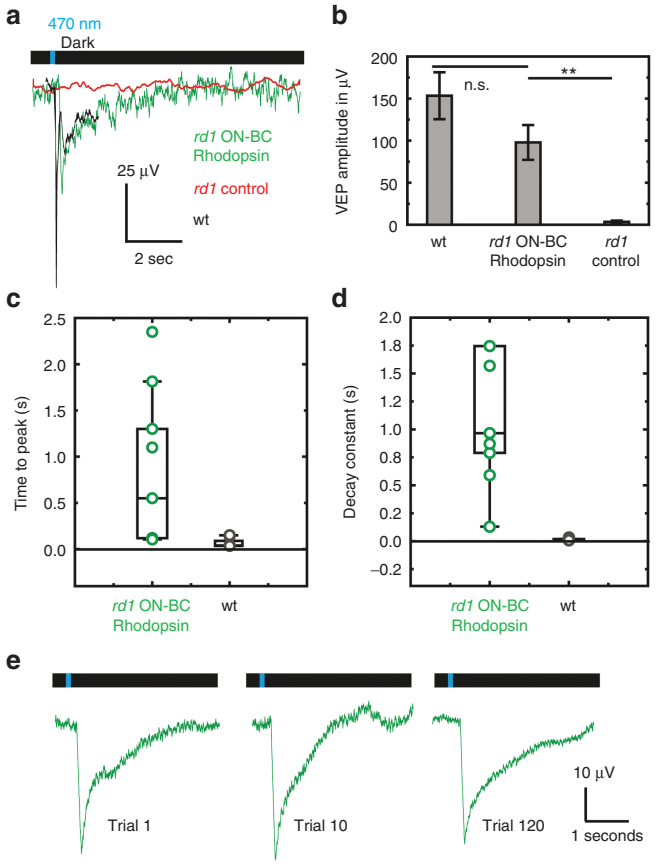

Figure 3 Rhodopsin activation in ON-BCs of *rd1* mice drives cortical responses *in vivo*. (**a**) Representative visually-evoked potential (VEP) traces from wild-type (black), *rd1* control (red), and ON-BC rhodopsin *rd1* mice in (green). Traces are averages of 15 sweeps in response to 100 ms flash of blue light (LED, 455 nm, 15 mW/cm^2). (**b**) Quantification of VEP peak amplitudes in response to 100 ms light pulse for wild-type mice (n = 5), ON-BC rhodopsin *rd1* (n = 9) and *rd1* control mice (n = 6). Data are means ± SEM. **P < 0.005, paired student's t-test. (**c,d**) Response kinetics for ON-BC rhodopsin *rd1* mice (n = 9) and wt mice (n = 7) with 100 ms stimulation at 455 nm. (**c**) Time from flash to peak response and (**d**) peak response decay constants are shown as combined boxplot (in black with mean, first and third quartile) and scatterplot (rhodopsin with green open circles, wt with black open circles). (**e**) Repeatability of VEP response over time in ON-BC rhodopsin *rd1* mice. Shown are three traces of the same animal in response to 100 ms stimulation with 20 seconds inter stimulus interval (ISI) taken at different time points (trials 1, 10, and 120).

Rhodopsin activation in ON-BCs drives cortical responses *in vivo*

We tested if rhodopsin-mediated signals in ON-BCs would propagate from the retina to higher visual areas in the brain by *in vivo* recording of local field potentials in the visual cortex of wild-type, control *rd1*, and rhodopsin-treated *rd1* mice. Mice were stimulated with pulses (100–1,000 ms) of light (455 nm, 15.0 mW/cm^2) delivered to the right eye using a fiber optic guide and VEPs were recorded in the contralateral primary visual cortex using an extracellular electrode. Starting at the dura, we slowly lowered the electrode until the light response reached the maximal amplitude, typically at a depth of 300–400 µm. Responses were recorded and averaged over 10–30 stimuli. Sham-injected *rd1* control mice (n = 6) had no measurable VEPs (**Figure 3a**,

red trace), consistent with the lack of functional photoreceptors, as shown in other studies.[12,16,19] In contrast, *rd1* mice expressing rhodopsin in ON-BCs (n = 8) (**Figure 3a**, green trace, and **Figure 3b**) had large VEPs, with amplitudes ~70% of that seen in wild-type mice (n = 5) (**Figure 3b**, black trace). We analyzed the kinetics of VEPs evoked by single 100 ms light pulses, given at long (60 seconds) intervals, and plotted the time to peak response and decay constant as a combined scatterplot and boxplot (n = 9 rhodopsin-treated mice, n = 7 wt mice) (**Figure 3c**,**d**). VEPs from rhodopsin treated *rd1* mice had slower response kinetics (time to peak: 0.84 ± 0.28 seconds, decay constant: 1.44 ± 0.29 seconds) when compared to wt mice (time to peak: 0.07 ± 0.02 seconds, decay constant: $0.02 \pm 3 \times 10^{-3}$ seconds) and these responses were more variable. Importantly, we found that light flashes in rhodopsin-treated *rd1* mice reliably triggered stable responses over dozens of stimuli presented to the same animal over a period of 1 hour of recording (**Figure 3e**). In order to determine if the low light intensities that we intended to use for subsequent mouse behavior would elicit robust responses *in vivo*, we recorded cortical responses from ON-BC rhodopsin treated *rd1* mice (n = 3) at low (0.1 mW/cm²) and high (1.5 mW/cm²) light intensities. In **Supplementary Figure S6a**, we show that low light stimulation elicited robust responses, with peak amplitudes approaching 50% of the response of high light stimulation, confirming that the low light levels can sufficiently activate rhodopsin *in vivo*.

Rhodopsin expression restores innate light avoidance and enables learned visually-guided behavior in *rd1* mice

Having established that rhodopsin expression in ON-BCs of *rd1* mice restored light responses to retinal explants *in vitro* and elicited cortical responses *in vivo*, we asked whether our treatment would also enable visually-guided behavior. To answer this question, we initially tested rhodopsin-treated *rd1* mice for light avoidance, a simple and robust behavior that is lost in *rd1* mice following the death of rod and cone photoreceptors.[13,21] Mice were habituated to a light/dark box (**Supplementary Figure S6b**) for 45 minutes together with their littermates and then tested for place preference individually in 5 minutes trials. The chamber was illuminated by a custom built LED array centered above the light side of the compartment (5 × 6 LED array, 445 nm, 0.1–0.2 mW/cm² at floor level). The time spent in the light and dark compartments was recorded on video and the percent time spent in the dark was calculated. Control mice (sham-treated *rd1* mice, n = 10) showed no preference for either compartment, as expected, whereas *rd1* mice expressing rhodopsin in ON-BCs (n = 16) displayed a strong, significantly enhanced light avoidance, which was indistinguishable from that of sham-injected wild-type animals (sham treated, n = 7) (**Supplementary Figure S6c**).

Next, we tested if rhodopsin-treated mice would overcome their innate light aversion by learning to associate light with a reward. We used a Y-maze variation of the Morris water maze (**Figure 4a**) and trained mice to find a submerged, hidden escape platform that was cued by uniform (nonpatterned) light, while the arm lacking the platform was dark.[13,33] Illumination in the arm containing the platform was produced by our 5 × 6 LED array (445 nm), which delivered 0.1 mW/cm² at the start of the

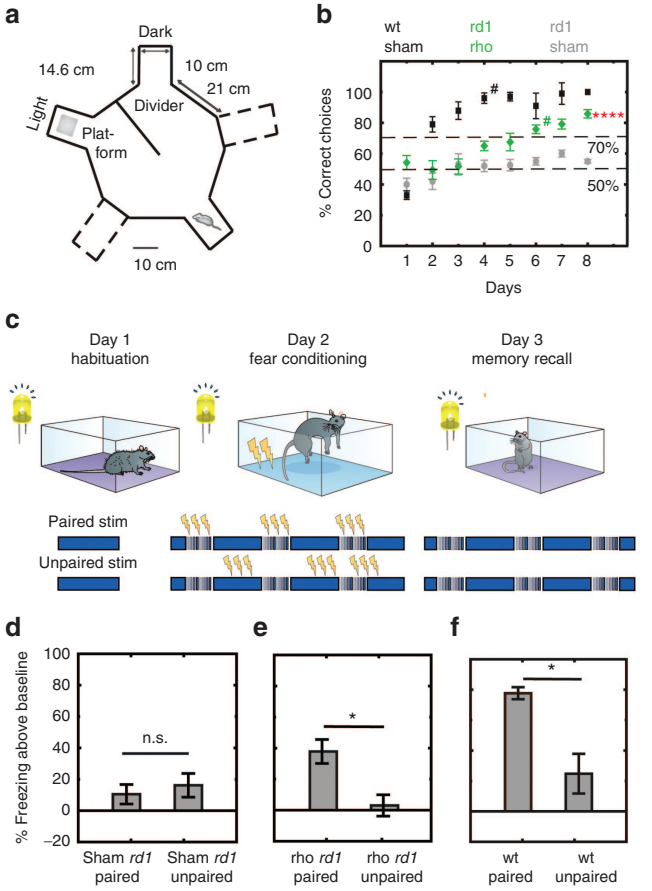

Figure 4 Rhodopsin expression restores innate light avoidance and enables learned visually guided behavior in *rd1* mice. (**a**,**b**) Forced two-choice associative learning task using a modified radial arm maze. (**c**) Schematic of the maze. (**d**) Performance of mice in y-maze over the course of 8 days. Percent correct choices are plotted for control *rd1* mice (gray, n = 6), ON-BC rhodopsin *rd1* (green, n = 6), and wild-type mice (black, n = 7). The dashed line at 50% indicates chance level while the 70% line indicates the threshold for pass (above) versus fail (below). # indicates the day at which all animals of one group have performed > 70% correct choices and thus learned the task. Data are means ± SEM. Statistics done on the performance of rhodopsin treated *rd1* mice and sham treated *rd1* control mice on day 8 show ****P < 0.00005 (445 nm, 100 µW/cm² at the divider, 1 mW/cm² at the platform). (**e**) Schematic for fear conditioning experiment. The blue bar represents the light stimulation (solid blue = non-patterned light, striped blue = spatial patterns) and flash icons represent 2-second footshocks. The paired paradigm is shown above; the unpaired shown below. (**f**,**g**,**h**) Quantification of fear response using spatially patterned stimulation. Percent freezing above baseline is shown for paired and unpaired paradigms for control *rd1* mice (n = 6 paired, n = 6 unpaired) (**f**), ON-BC rhodopsin *rd1* (n = 8 paired, n = 8 unpaired) (**g**) and wild-type mice (n = 6 paired, n = 6 unpaired) (**h**). Data are means ± SEM. *P < 0.05 (light intensity at the floor level 0.1–0.2 mW/cm²).

divider, and 1 mW/cm² at the platform (**Figure 4a**). Mice were habituated to the maze for 2 days prior to training (see Methods) and then subjected to 20 trials per day for 8 consecutive days. Their behavior was recorded on video and the performance was subsequently analyzed. Trials in which the mouse swam to the platform at the end of the illuminated arm of the maze without entering the dark arm were categorized as successes. Trials in which the mouse explored the dark arm first or took longer than 60 seconds to reach the platform were scored as failures. As in

previous work,[13,33] mice were considered to have learned the task when the performance was equal or above 70% correct choices. Control mice (sham-treated *rd1* mice, $n = 6$) were able to improve their performance over the course of the experiment, but did not reach the threshold required for passing the test, which is in good agreement with earlier studies[13,33] (but see ref. 34). R*d1* mice that expressed rhodopsin in ON-BCs ($n = 6$) showed improvement after 4 days and reached the 70% learning threshold after 6 days of training (**Figure 4b**, green pound sign). Treated mice performed significantly better than controls on day 8 (**Figure 4b**). Wild-type mice (sham treated, $n = 7$) improved after day 1 and had learned the task by day 4 (**Figure 4b**, black pound sign).

Finding that rhodopsin expression in ON-BCs enabled *rd1* mice to distinguish light from dark, we next tested their ability to recognize and distinguish between distinct light patterns (moving versus static spatial patterns) in the context of the visually cued fear-conditioning paradigm. In this paradigm, mice learn to associate electric foot shocks with light cues. We followed the protocol described by Tochitsky *et al.*[18] with slight modifications. Mice were habituated to the chamber on day 1, conditioned on day 2 and tested for memory recall on day 3 (**Figure 4c**). Constant illumination of the chamber was provided by a static light pattern, consisting of a vertical bar that was generated by illumination of a single vertical row in a 5×6 LED array (0.1 mW/cm^2). We cued the foot shocks by switching from this static pattern to a dynamic pattern in which the single vertical row progressed horizontally at a speed that completed a cycle in 0.6 seconds (1.66 Hz refresh rate). The static and moving bars had equal luminescence. During the conditioning phase, a 10-second presentation of the dynamic pattern (blue stripes in **Figure 4c**) was paired with short 2 seconds foot shocks (indicated by flash icons in **Figure 4c**). For memory recall, the same pattern of lights was presented without the shocks. The mice were filmed during the recall period and freezing behavior was scored using FreezeFrame software (Coulbourne Instruments, PA). For the unpaired condition, mice were presented with the same number of moving patterns and shocks presented in a random sequence. We tested sham-injected *rd1* control mice, rhodopsin treated mice and wt mice and subdivided each into two groups, one which received the paired stimulation and the other which received the unpaired stimulation. The videos taken during recall were analyzed and percent freezing above baseline (percent freezing after—before light cue) was plotted. Sham-treated *rd1* mice ($n = 6$ per group) showed freezing behavior to the cue but it was not significantly different between paired and unpaired conditions (**Figure 4d**). Rhodopsin-treated *rd1* mice ($n = 8$ per group), however, displayed robust freezing behavior in response to the moving pattern (**Figure 4e**), similar to the level seen in wt mice ($n = 6$ per group) (**Figure 4f**).

DISCUSSION

Gene therapy approaches to treat retinal diseases have experienced a tremendous expansion in recent years, with ongoing clinical trials for several retinal dystrophies, including Leber congenital amaurosis type 2, Usher syndrome type 1B, Stargardt's disease neovascular age-related macular degeneration and choroideremia,[35] all of which fall under the category of gene replacement or augmentation therapies. Optogenetic gene therapies are still in the process of testing and optimization in animal models of human blindness. Before moving to the clinic, major challenges have to be addressed and overcome.

In this study, we solved a major challenge of optogenetic gene therapy for blindness by introducing a native opsin of the mammalian retina, the light-gated GPCR rhodopsin, as an optogenetic actuator, which we found to provide orders of magnitude of enhancement in light sensitivity over the microbial opsin channelrhodopsin. We delivered rhodopsin to blind mice via intravitreal injection of a viral vector containing a cell-specific promoter and showed efficient, cell-specific expression in ON-BCs. We demonstrated that retinal explants expressing rhodopsin in ON-BCs respond to extremely low light intensities with moderately fast kinetics. *In vivo* cortical recordings also showed high sensitivity to light and were reproducible over extended periods of time, suggesting sufficient retinal recycling. Finally, we found that delivery of the rhodopsin gene to ON-BCs both restored innate light avoidance and enabled learned behavior that depended on mice distinguishing between light and dark or between static and moving spatial light patterns.

Several recent studies[12,14–16] have focused on ON-BCs as retinal gene therapy targets. ON-BCs are appealing target neurons, since they are upstream in the retinal circuitry, providing an opportunity to preserve some aspects of retinal processing.[11,25] Depolarization of ON-BCs with optogenetic actuators can generate both ON and OFF responses in downstream RGCs, reminiscent of the wild-type retinal circuitry. Importantly for our study, ON-BCs have a GPCR-mediated signal transduction pathway that is triggered by glutamate, released by photoreceptor cells, acting on the ON-BC metabotropic glutamate receptor, mGluR6, and its apparent downstream effector, the TrpM1 channel.[27] Our promoter element, which is based on the mGluR6 promoter, is selective for ON-type bipolar cells but does not distinguish between cone and rod bipolar cells. To investigate the contribution of cone versus rod bipolar cells, we costained treated retinas with the rod bipolar cells marker PKC-α and looked a colocalization of YFP and PKC-α. Our findings shown in **Supplementary Figures S1 and S2** suggest that while some cone ON-BCs express rhodopsin-YFP, rod bipolar cells comprise over 2/3 of all virally transduced bipolar cells, consistent with other recent studies.[15]

Our hope was that rhodopsin would operate as a more sensitive optogenetic actuator than prior optogenetic treatments,[10,12,14,17,19,20] which require very high light intensities, intensities that are potentially toxic to any remaining photoreceptors and other retinal cells.[36] Our intensity-response curves from *rd1* mice expressing rhodopsin in ON-BCs recorded *in vitro* showed strikingly high light sensitivity, similar to what was reported in another study that employed light-gated GPCRs targeted to ON bipolar cells.[37] Recent studies by other groups have reported a wide range of threshold light intensities needed to drive a response in retinas of *rd1* mice expressing ChR2 in ON-BCs.[14–16] These values could not be readily compared to our results with rhodopsin due to differences in light delivery, ChR2 variant, viral vector, cell-specific promoter, and functional measurement. We therefore compared rhodopsin to one of the most widely used enhanced ChR2 variants, H134R, and did so under identical conditions of promoter, viral construct, intravitreal viral delivery, light exposure, and

outcome measure. Under these identical conditions, using the most easily quantified MEA measurements, the lowest tested light intensities that evoked reliable responses in rhodopsin expressing retinas was 1,000-fold lower than the threshold intensity required to elicit a response in ChR2-expressing retinas. It is important to note that the minimal intensity that was tested with rhodopsin elicited robust responses (18% normalized firing rate), suggesting an even lower threshold and larger advantage over ChR2.

It is important to consider that rhodopsin responded to a very broad range of intensities, spanning ~5 log units, whereas ChR2 had a narrow response range of ~2 log units. The rhodopsin sensitivity curve was fit with a Hill-type function (data not shown) that was best described by a sigmoidal curve. Dose–response relationships arise from complex interactions of multiple molecular factors and cellular functions and are thus hard to interpret. Wild-type retinas by comparison respond within a range of ~2 log units, but their sensitivity is adjusted by adaptation and contrast gain control. Late-stage retinal degeneration patients, who have few or no surviving photoreceptors may have lost much of their light adaptation, making a wide response range of the optogenetic actuator to luminance desirable, although it could mean a compromised detection of contrast, since a significant change in light intensity does not induce a significant change in firing rate (**Figure 2c**). This could be corrected with external hardware for user implementation.

In vivo measurements of light sensitivity in *rd1* mice expressing rhodopsin in ON-BCs also showed very high sensitivity. Visually-evoked activity in primary visual cortex was evoked by dim light flashes and visually-guided behavior experiments were successfully performed at very dim light levels (0.1–0.2 mW/cm^2). The behavioral light intensity was measured using VEP in the primary visual cortex to ensure that the *in vivo* response was sufficient for driving complex behavior (**Supplementary Figure S6a**). A quantitative comparison of *in vitro* and *in vivo* sensitivity is not possible due to lens optics, differences in light sources and stimulating wavelength (510 nm *in vitro* versus 445–455 nm *in vivo*), cell populations and experimental setup, but all the experiments described here support the notion that GPCRs generate substantially greater light sensitivity when compared to single ion channels.

Typically, there is a tradeoff between speed and sensitivity of optogenetic actuators, whereby the more sensitive systems function at slower rates. In the case of ion channels (*e.g.*, channelrhodopsin or halorhodopsin), the light sensor (opsin), and the effector (channel) are the same molecule, whereas GPCR cascades separate the sensor (opsin) and the effector (channel) functions. This separation allows for adaptation and regulation of the circuit, but the additional components and their individual kinetics are additive, resulting in a slower overall signal transduction mechanism. In addition, the proteins and processes evolved to rapidly terminate the light response in rod photoreceptors (rhodopsin kinase and arrestin[38]) are not found in ON-BCs, significantly slowing down the return from the light activated to the dark adapted state. We characterized the kinetics of the rhodopsin-mediated signal *in vitro* and *in vivo* and found average decay constants ranging between 1.2 (**Figure 2d**) and 0.97 seconds (**Figure 3d**). With varying stimulating light intensities, however, the kinetics shifted, and both time to reach peak as well as the time to reach baseline increased with decreasing light intensities (**Figure 2e,f**). The notion that ON kinetics should be a function of light intensity is intuitive, whereas the mechanism for light dependent decay is more surprising. Cortical measurements *in vivo* (**Figure 3c,d**) matched closely with those *in vitro* and confirmed that both on and off kinetics were in the 1–3-second range for moderate light intensities and in the sub-second range for high light intensities. This is a great improvement over previous studies using melanopsin.[13] Recent work using cone opsins has indicated that they may be inherently faster,[39] providing a potential strategy to further improve kinetics.

In this study, we did not report on the OFF response but on the inhibition of spontaneous firing by light. This was quantified in the calculation of photoswitching index as the firing rate during the light stimulus divided by the firing rate before light stimulation (as reported in **Supplementary Figure S5d**). The negative photoswitching index values suggest that lateral circuitry upstream of the RGCs may be involved in our signaling pathway but is not identical with an OFF response. Contrary to our expectations and to findings from recent studies,[15,16] rather few cells were found to have a negative photoswitching index. Multiple factors may contribute to this. We stimulated retinas with a nonpatterned, full-field flash of light, illuminating the entire retina at once—a stimulus that may elicit excitation that out-competes lateral inhibition in the upstream circuitry. Furthermore in "treated" *rd1* retinas, rhodopsin expression may be too sparse, or light-activated currents too low (*i.e.*, on the level reached by Lagali *et al.*[12] and Doroudchi *et al.*[14]) to drive a lateral circuitry capable of producing inhibition that we can detect using the photoswitching index.

To test if rhodopsin treatment could provide useful visual information for mice, we tested their ability to perform visually guided behavior tasks. We found that rhodopsin expression restored innate light avoidance in the open-field test. However, in a subsequent experiment, we found that treated mice could also learn to overcome this aversion and associate light with reward using a Y-maze task. Importantly, a visual prosthetic should allow basic forms of spatial and temporal pattern recognition. To test spatial pattern recognition, we conditioned mice to associate a marching bar of LEDs with electric foot shocks and distinguish this stimulus from an intensity matched static decoy stimulus (still LED bar). We tested the ability of mice to recall this association and were able to demonstrate that rhodopsin expression in ON-BC-enabled mice to detect and distinguish dynamic light stimuli from static decoy stimuli. While we have not yet tested temporal pattern recognition, our kinetics analysis (**Figure 2d–f** and **Figure 3g**) predicts that treated mice can resolve frequencies of ~1Hz. While these behavioral experiments provide evidence that rhodopsin treated mice can detect and distinguish basic patterns of light from nonpatterned light, we currently do not know the spatial or temporal resolution that treated mice can resolve and we have not yet tested shape discrimination (*i.e.*, distinction between two static patterns). These experiments are important future directions that will require head-fixed preparations instead of free viewing conditions presented in this study.

Rhodopsin-mediated signals showed a high amount of variability between cells and retinas *in vitro and in vivo* (**Figures 2e,f**

and 3c,d), but are consistent in their response characteristics over time. Cortical VEP responses over >120 trials (Figure 3e) indicated stable functioning of the GPCR and the visual retinoid cycle. Despite trial-to-trial stability, the response properties covered a wide range (time to peak and decay constant Figure 3c,d), indicating that other factors might play a role in variability. The non-linearity introduced by the GPCR, saturation of G-protein levels within the cell, differential expression of G-protein gated channels for different subsets of ON-BCs as well as the degeneration state of the retina are all likely to contribute to the observed variability. In wild type photoreceptors, light triggers rhodopsin to activate the G-protein transducin (G_T), which in turn leads to closure of cyclic GMP-gated channels and subsequently hyperpolarizes the cell.[22] Exogenously-expressed rhodopsin is known to be promiscuous and can activate $G_{i/o}$ in the absence of G_T[40] and is therefore functional in many different contexts such as HEK cells and C-elegans.[40,41] Surprisingly, in our experiments, rhodopsin activation lead to light-induced depolarization of ON-BCs. Rhodopsin's ability to "hijack" preexisting messaging systems and function at low light levels via amplification may be more widely applicable. Future work will be needed to determine the identity of the signaling mechanism that leads to this light dependent depolarization. Independent of the molecular mechanism, however, it is important to note that our approach is favorable for clinical application for multiple reasons. First, the risk for immunoreactivity is reduced due to use of a retina native mammalian protein; second, intravitreal virus injections used in our approach are technically easy to perform and have a high success rate; third, our system couples to the bioavailable ligand retinal avoiding the need for recurrent chemical treatment, and fourth, improved sensitivity allows for low light stimulation, preventing further damage to remaining photoreceptors of patients undergoing treatment.

In summary, we have presented an optogenetic approach for a retinal prosthesis that is: (i) native to the retina, (ii) far more sensitive than other optogenetic treatments, and (iii) potentially safer for human applications since it circumvents the need for microbially derived proteins.

MATERIALS AND METHODS

Animals. University of California Animal Care and Use Committee approved all mouse experiments. Wt mice (C57Bl/6J) and *rd1* mice (C3H) were purchased from Jackson Laboratory (Bar Harbor, ME) and injected with rAAV between p30-p60 and used for *in vivo* and *in vitro* experiments between p90-p160. Transgenic grm6-EGFP mice were a kind gift from Noga Vardi. All mice were housed on a 12-hour light dark cycle with food and water *ad libitum*.

Packaging and injection of rAAV. Adeno-associated viruses were made using via standard procedures.[42] The Rho construct (origin is rat) with the rAAV2/2(4YF) capsid carried the vertebrate rhodopsin transgene tagged C-terminally[31] with yellow fluorescent protein and controlled control by the 4× repeat of the metabotropic glutamate receptor 6 promoter (4xgrm6). The ChR2 construct was also packed with the rAAV2/2(4YF) capsid carrying the humanized version of the ChR2 (H134R) transgene tagged C-terminally with yellow fluorescent protein under the control of the 4xgrm6 promoter. The titer of AAVs was determined via qPCR relative to inverted repeat domains standard. Titers for these viruses ranged between 1×10^{13} and 1×10^{14} vg/ml. Mice were anesthetized with IP ketamine (72 mg/kg) and xylazine (64 mg/kg). Eyes were anesthetized with proparacaine (0.5%) and pupils were dilated with phenylephrine (2.5%) and tropicamide (1%). During the injection procedure, an incision was made posterior of the ora serrata using a sharp 30-gauge needle. A 2 µl volume containing an estimated amount of 5×10^{11} viral genomes of AAV diluted in phosphate-buffered saline (PBS) (with 1% phenol red as contrast agent) was then fed through the incision site and injected intravitreally using a blunt 32-gauge Hamilton syringe (Reno, NV). Hamilton needle tip was left in the eye for >60 seconds to allow homogenization and reduce the efflux.

Tissue preparation and immunohistochemistry. Mice were sacrificed >6 weeks after AAV injection and the eyes were enucleated and fixed in 4% paraformaldehyde (Ted Pella) for 1 hour. Using scissors, the cornea was removed by making a circular incision around the ora serrata. Placing two forceps around the edges of the eyecup and genteelly tearing separates the retina from the sclera. Radial cuts were made to flatten the retina in forming the typical clover-leaf shape. For retinal sections, wholemounts were embedded in agarose (Sigma, St Louis, MO) and transverse sections were taken using a vibratome (Leica, Mannheim, Germany) at medium speed, maximum vibration and 150 µm thickness.

Wholemounts and sections were incubated in blocking buffer (10% normal goat serum, 1% bovine serum albumin, and 0.5% Triton X-100 in PBS (pH 7.4)) for 2 hours at RT. Primary antibodies were applied over night at 4 °C with the following dilutions: PKC-α (Rabbit monoclonal (Y124), Abcam, 1:1,000), ChAT (Rabbit polyclonal, AB143, Millipore, 1:500). The secondary antibody (Alexa-594 anti-rabbit, Invitrogen, Carlsbad, CA) was applied at 1:1,000 for 2 hours at RT. After three 10 minutes PBS washes, tissue was mounted on slides using Vectashield (Vector labs, Burlingame) mounting medium with DAPI (4',6-diamidino-2-phenylindole) to stain cell nuclei. Wholemounts and sections were imaged using a confocal microscopy (LSM7, Carl Zeiss, Gottingen, Germany). Lasers and channels were assigned using the "best signal" option to ensure there was no spectral overlap between them. Sections were imaged as z-stacks with 2 µm step size and rendered as maximum projections for export. Wholemounts were imaged as optical sections in a single plane. Images were averaged over four repeated scans and the scanning speed was adjusted according to expression levels. Brightness and contrast was adjusted using ZEN imaging software (Carl Zeiss, Gottingen, Germany), and images were exported as TIFF. Scalebars were added using Adobe Photoshop. Finally, software assisted colocalization was performed using the built-in confocal imaging software ZEN (Carl Zeiss, Gottingen, Germany) and thresholds were adjusted manually according to the pixel intensity distribution.

MEA recordings. MEA recordings were performed on treated and untreated *rd1* mice as well as untreated wt (C57Bl/6J) mice. Control mice and wt mice were used at age >p90. Experimental mice were used 6–10 weeks following AAV injection. The excised retina was placed ganglion cell side down[43] in the recording chamber (pMEA 100/30iR-Tpr, Multi Channel Systems, Reutlingen, Germany) of a 60-channel multi electrode array system and constant with constant vacuum pump (perforated MEA1060 system with CVP; Multi Channel Systems, Reutlingen, Germany). A mesh weight (Scientific Instruments - Slice grids) was placed on the retina to improve electrode contact and signal-to-noise. In some instances, vacuum was also applied to the base of the retina (Multi Channel Systems vacuum system). During recording, a constant perfusion of oxygenated Ames media (32 °C) was provided to the recording chamber. Recordings lasted between one to two hours. Illumination coupled to a 4× objective and produced using a 300 W mercury arc lamp (DG-4, Sutter Instruments, Novato, CA) with a green band pass filter (510/50 nm, Thorlabs, Newton, NJ). All light intensities reported were measured with a handheld power meter (Thorlabs). Data were sampled at 25 kHz filtered between 300–2,000 Hz and recorded using MCS rack software (Multi Channel Systems, Reutlingen, Germany) for off-line analysis. Voltage traces were converted to spike trains off-line by collecting responses using methods described below. Spikes recorded

at one electrode were sorted into single units, which we defined as "cells", via principal components analysis using Offline Sorter (Plexon, Dallas, TX). Single unit spike clusters were exported to MatLab and analyzed and graphed with custom software. Putative ipRGC cells that responded for more than 30 seconds after termination of light stimulus were excluded from analysis. For extracting firing rates in the dark, the 3-second preceding flash were averaged to minimize fluctuations. The firing rates in the light were taken as peak response during the light stimulation. Photoswitching index PI was calculated using the formula (firing rate light - firing rate dark)/(firing rate light + firing rate dark). Cells were considered responsive if PI > 0.1 or PI < −0.1. All cells per figure are from the same retina unless otherwise specified. Two methods were used for setting the threshold for spikes: (i) For raster plots (**Figure 2a,b**), the baseline for each cell was set at a threshold just above electrical noise to include all possible spikes and provide a more global perspective. (ii) For plots that show changes in firing rate due to light intensity (**Figure 2c,e,f**), the thresholds were set to include all responding cells (PI > 0.1 or PI < −0.1). Peri-stimulus time histograms of every cell were correlated with one another.

Recording of VEPs. Adult *rd1* and wt mice were anesthetized using chlorprothixene (2 mg/kg, intraperitoneally) and urethane (1.5 g/kg, intraperitoneally) and supplemented with 0.5–1% isoflurane for the first 30 minutes. Body temperature was maintained throughout the experiment using a DC temperature controller and a heating pad (FHC, Bowdoin, ME). Pupils were dilated with tropicamide (1%) and a small headplate was attached. A small craniotomy and durotomy was made over the primary visual cortex (1.7 mm lateral to midline and 0.7 mm anterior to lambda). Electrodes with a resistance of 3 MΩ were pulled from borosilicate glass (1.5 mm OD, 1.16 mm ID, Warner Instruments, Hamden, CT) using a horizontal puller (Sutter Instruments, Novato, CA). Electrodes were filled with ACSF (124 mmol/l NaCl, 2.5 mmol/l KCl, 2.0 mmol/l $MgSO_4$, 1.25 mmol/l KH_2PO_4, 26 mmol/l $NaHCO_3$, 10 mmol/l glucose, 4 mmol/l sucrose, 2.5 mmol/l $CaCl_2$ all purchased from Sigma), placed over the craniotomy and slowly lowered to a final depth of 400 µm, to layer 4 of the visual cortex. The contralateral eye was stimulated using 100–1,000 ms pulses of blue light (455 nm, 15 mW/cm^2) and responses were recorded using the Axoclamp 200B amplifier (Axon Instruments, Foster City, CA). For each condition, 20–100 sweeps were recorded at 10 kHz, filtered at 2 kHz and analyzed with custom software in MatLab.

Open-field test. The open-field test was performed as described previously,[13,21] with minor modifications, see **Supplementary Figure S6b**. Briefly, a plastic box (dimensions l = 60 cm, *w* = 40 cm, *h* = 30 cm) was divided into a light compartment (l = 25 cm, *w* = 40 cm, *h* = 30 cm) with white walls and a dark compartment (l = 35 cm, *w* = 40 cm, *h* = 30 cm) with black walls. The light compartment was illuminated by a custom LED array (5×6 LEDs, 447.5 nm Rebel LED, Luxeon star, Brantford, Canada) centered over the compartment. The light intensity was 100–200 µW/cm^2 at the bottom of the box. A small opening allowed the mice to move between the two compartments (*h* = 5 cm, *w* = 10 cm). Mice were brought into the testing room in their home cages, transferred to the open-field box with their littermates and allowed to habituate to the new environment for 45 minutes. Mice were placed back in their home cage then tested individually. Mice were placed in the light compartment and were given a maximum of 3 minutes to discover that there is a second compartment. A 5-minute trial began when they crossed into the dark compartment, and time spent in the light was recorded. Mice that crossed the opening only once and stayed in the dark compartment for entire time were disqualified. Permanent records were made using a video camera (GoproHero3).

Forced 2-choice water maze task. The water maze task was performed using the protocol described by Wong *et al.*[33] and Gaub *et al.*[21] with minor modifications. A radial arm maze was modified into a forced two choice task by blocking two of the five arms of the maze (**Figure 4c**) and adding a divider (dimensions: 25×25 cm) to separate the two potential "escape arms". A custom built LED array (5×6 LEDs, 447.5 nm Rebel LED, Luxeon star) was placed at the end of one of the "escape arms" cuing the escape platform. The light intensities at the divider (0.1 mW/cm^2) and (1 mW/cm^2) were measured at the water level using a handheld power meter (Thorlabs).

Light cued fear conditioning. Fear conditioning experiments were performed using Colbourn shock chambers-Colbourn Habitest chamber with test cage (Coulbourn Instruments, PA). Control *rd1* and wt mice were sham (PBS) injected prior the experiment to control for the virus treatment. On the first day, animals were brought into the testing room in their home cages and then individually acclimated to clean Colbourn shock chambers (Coulbourn Instruments) for 30 minutes. On the second day, animals received training. Mice were subjected to paired or unpaired light cued fear conditioning, consisting of 5 minutes habituation to the chamber with "non-patterned lights-on" followed by three cued shock trials at 0.7 mA. For paired trials, the 20-second "patterned lights-on" cue conincided with 3×2-second footshocks at 4 seconds intershock-interval. Intertrial interval was 40 seconds. For unpaired trials, animals received the same amount of footshocks and the same time of patterned light cue but the footshocks occured independent from the light cue. These brief, low current shocks provided the minimal aversive stimuli to create a fearful memory associated with patterned light (custom built LED array with 5×6 LEDs, 447.5 nm Rebel LED, Luxeon star) with moving bar (one row at a time) with a 600 ms cycle, 100–150 µW/cm^2). On the third day, animals were tested in a fear probe trial. Thefloor to deliver footshocks was replaced with a solid floor. Mice were habituated to the chamber for 5 minutes, and subjected to the same light stimulation protocol as on day 2, but without shock, while being recorded by Colbourn's FreezeFrame software. The recordings were used to analyze conditioned fear behavior (time spent freezing, a typical rodent fear response) associated with the learned light cue.

Statistical analysis. The Students' *t*-test was used for statistical analysis of *in vivo* mouse physiology (**Figures 3** and **4**).

SUPPLEMENTARY MATERIAL

Figure S1. Targeted expression of rhodopsin in ON-bipolar cells of *rd1* mouse retina.
Figure S2. Co-localization of virally expressed rhodopsin-YFP with rod bipolar cell marker PKC alpha.
Figure S3. Targeted expression of Channelrhodopsin2 in ON-bipolar cells of *rd1* mouse retina.
Figure S4. Co-localization of virally expressed ChR2-YFP with rod bipolar cell marker PKC alpha.
Figure S5. Characterization of rhodopsin-mediated signals.
Figure S6. Quantification and schematic of light/dark box test.

ACKNOWLEDGMENTS

We thank Botond Roska and Connie Cepko for providing the 4xgrm6 promoter; Hillel Adesnik for teaching the VEP technique and providing the instruments; Aaron Friedman and Daniela Kaufer for fear conditioning training and equipment; Meike Visel for preparation of AAV; Gautam Agarwal and Drew Friedmann for design of custom MATLAB analysis software; Andreas Reiner, Josh Levitz, Reza Vafabahsh, and Chris Fortenbach for discussion and editing of manuscript; Frank Werblin, Marie Burns, and Edward Pugh for helpful advice; Matthew Anderson for help with custom LED light source; Holly Aaron and the UC Berkeley Molecular Imaging Center for help with microscopy; Fulbright foundation for supporting Benjamin Gaub. This work was funded by NIH Nanomedicine Development Center for the Optical Control of Biological Function (PN2EY018241), RO1EY06855; P30EY-001583 and the Foundation Fighting Blindness, USA. J.G.F. and E.Y.I. supervised the project. B.M.G performed intraocular AAV injections, cortical recordings (VEP) and retinal histology in mouse. M.H.B. and B.M.G performed mouse multi electrode array recordings and

data analysis. A.E.H., M.H.B., and B.M.G performed mouse behavior. B.M.G., M.H.B., E.Y.I., and J.G.F. wrote the manuscript. All authors reviewed the manuscript. E.Y.I. is an author on US Patent No. US 8,114,843 B2 on the design of protein photoswitches and a co-founder of Photoswitch Biosciences, Inc., which employs such switches in cell-based assays for drug screening.

REFERENCES

1. Haverkamp, S, Michalakis, S, Claes, E, Seeliger, MW, Humphries, P, Biel, M *et al.* (2006). Synaptic plasticity in CNGA3(-/-) mice: cone bipolar cells react on the missing cone input and form ectopic synapses with rods. *J Neurosci* **26**: 5248–5255.
2. Marc, RE, Jones, BW, Watt, CB and Strettoi, E (2003). Neural remodeling in retinal degeneration. *Prog Retin Eye Res* **22**: 607–655.
3. Mazzoni, F, Novelli, E and Strettoi, E (2008). Retinal ganglion cells survive and maintain normal dendritic morphology in a mouse model of inherited photoreceptor degeneration. *J Neurosci* **28**: 14282–14292.
4. Santos, A, Humayun, MS, de Juan, E Jr, Greenburg, RJ, Marsh, MJ, Klock, IB *et al.* (1997). Preservation of the inner retina in retinitis pigmentosa. A morphometric analysis. *Arch Ophthalmol* **115**: 511–515.
5. Bainbridge, JW, Smith, AJ, Barker, SS, Robbie, S, Henderson, R, Balaggan, K *et al.* (2008). Effect of gene therapy on visual function in Leber's congenital amaurosis. *N Engl J Med* **358**: 2231–2239.
6. Maguire, AM, High, KA, Auricchio, A, Wright, JF, Pierce, EA, Testa, F *et al.* (2009). Age-dependent effects of RPE65 gene therapy for Leber's congenital amaurosis: a phase 1 dose-escalation trial. *Lancet* **374**: 1597–1605.
7. Shintani, K, Shechtman, DL and Gurwood, AS (2009). Review and update: current treatment trends for patients with retinitis pigmentosa. *Optometry* **80**: 384–401.
8. Humayun, MS, Dorn, JD, da Cruz, L, Dagnelie, G, Sahel, JA, Stanga, PE *et al.*; Argus II Study Group. (2012). Interim results from the international trial of Second Sight's visual prosthesis. *Ophthalmology* **119**: 779–788.
9. Zrenner, E, Bartz-Schmidt, KU, Benav, H, Besch, D, Bruckmann, A, Gabel, VP *et al.* (2011). Subretinal electronic chips allow blind patients to read letters and combine them to words. *Proc Biol Sci* **278**: 1489–1497.
10. Bi, A, Cui, J, Ma, YP, Olshevskaya, E, Pu, M, Dizhoor, AM *et al.* (2006). Ectopic expression of a microbial-type rhodopsin restores visual responses in mice with photoreceptor degeneration. *Neuron* **50**: 23–33.
11. Busskamp, V, Duebel, J, Balya, D, Fradot, M, Viney, TJ, Siegert, S *et al.* (2010). Genetic reactivation of cone photoreceptors restores visual responses in retinitis pigmentosa. *Science* **329**: 413–417.
12. Lagali, PS, Balya, D, Awatramani, GB, Münch, TA, Kim, DS, Busskamp, V *et al.* (2008). Light-activated channels targeted to ON bipolar cells restore visual function in retinal degeneration. *Nat Neurosci* **11**: 667–675.
13. Lin, B, Koizumi, A, Tanaka, N, Panda, S and Masland, RH (2008). Restoration of visual function in retinal degeneration mice by ectopic expression of melanopsin. *Proc Natl Acad Sci USA* **105**: 16009–16014.
14. Doroudchi, MM, Greenberg, KP, Liu, J, Silka, KA, Boyden, ES, Lockridge, JA *et al.* (2011). Virally delivered channelrhodopsin-2 safely and effectively restores visual function in multiple mouse models of blindness. *Mol Ther* **19**: 1220–1229.
15. Cronin, T, Vandenberghe, LH, Hantz, P, Juttner, J, Reimann, A, Kacsó, AE *et al.* (2014). Efficient transduction and optogenetic stimulation of retinal bipolar cells by a synthetic adeno-associated virus capsid and promoter. *EMBO Mol Med* **6**: 1175–1190.
16. Macé, E, Caplette, R, Marre, O, Sengupta, A, Chaffiol, A, Barbe, P *et al.* (2015). Targeting channelrhodopsin-2 to ON-bipolar cells with vitreally administered AAV Restores ON and OFF visual responses in blind mice. *Mol Ther* **23**: 7–16.
17. Polosukhina, A, Litt, J, Tochitsky, I, Nemargut, J, Sychev, Y, De Kouchkovsky, I *et al.* (2012). Photochemical restoration of visual responses in blind mice. *Neuron* **75**: 271–282.
18. Tochitsky, I, Polosukhina, A, Degtyar, VE, Gallerani, N, Smith, CM, Friedman, A *et al.* (2014). Restoring visual function to blind mice with a photoswitch that exploits electrophysiological remodeling of retinal ganglion cells. *Neuron* **81**: 800–813.
19. Caporale, N, Kolstad, KD, Lee, T, Tochitsky, I, Dalkara, D, Trauner, D *et al.* (2011). LiGluR restores visual responses in rodent models of inherited blindness. *Mol Ther* **19**: 1212–1219.
20. Tochitsky, I, Banghart, MR, Mourot, A, Yao, JZ, Gaub, B, Kramer, RH *et al.* (2012). Optochemical control of genetically engineered neuronal nicotinic acetylcholine receptors. *Nat Chem* **4**: 105–111.
21. Gaub, BM, Berry, MH, Holt, AE, Reiner, A, Kienzler, MA, Dolgova, N *et al.* (2014). Restoration of visual function by expression of a light-gated mammalian ion channel in retinal ganglion cells or ON-bipolar cells. *Proc Natl Acad Sci USA* **111**: E5574–E5583.
22. Arshavsky, VY and Burns, ME (2014). Current understanding of signal amplification in phototransduction. *Cell Logist* **4**: e29390.
23. The Lasker/IRRF Initiative for Innovation in Vision Science (2014). Restoring vision to the blind: The Lasker/IRRF initiative for innovation in vision science. *Trans Vis Sci Tech* **3**: 1.
24. Vinores, SA, Küchle, M, Derevjanik, NL, Henderer, JD, Mahlow, J, Green, WR *et al.* (1995). Blood-retinal barrier breakdown in retinitis pigmentosa: light and electron microscopic immunolocalization. *Histol Histopathol* **10**: 913–923.
25. Busskamp, V, Picaud, S, Sahel, JA and Roska, B (2012). Optogenetic therapy for retinitis pigmentosa. *Gene Ther* **19**: 169–175.
26. Busskamp, V and Roska, B (2011). Optogenetic approaches to restoring visual function in retinitis pigmentosa. *Curr Opin Neurobiol* **21**: 942–946.
27. Shen, Y, Heimel, JA, Kamermans, M, Peachey, NS, Gregg, RG and Nawy, S (2009). A transient receptor potential-like channel mediates synaptic transmission in rod bipolar cells. *J Neurosci* **29**: 6088–6093.
28. Sancho-Pelluz, J, Arango-Gonzalez, B, Kustermann, S, Romero, FJ, van Veen, T, Zrenner, E *et al.* (2008). Photoreceptor cell death mechanisms in inherited retinal degeneration. *Mol Neurobiol* **38**: 253–269.
29. Dalkara, D, Byrne, LC, Klimczak, RR, Visel, M, Yin, L, Merigan, WH *et al.* (2013). In vivo-directed evolution of a new adeno-associated virus for therapeutic outer retinal gene delivery from the vitreous. *Sci Transl Med* **5**: 189ra76.
30. Petrs-Silva, H, Dinculescu, A, Li, Q, Deng, WT, Pang, JJ, Min, SH *et al.* (2011). Novel properties of tyrosine-mutant AAV2 vectors in the mouse retina. *Mol Ther* **19**: 293–301.
31. Moritz, OL, Tam, BM, Papermaster, DS and Nakayama, T (2001). A functional rhodopsin-green fluorescent protein fusion protein localizes correctly in transgenic Xenopus laevis retinal rods and is expressed in a time-dependent pattern. *J Biol Chem* **276**: 28242–28251.
32. Lamb, TD (1995). Photoreceptor spectral sensitivities: common shape in the long-wavelength region. *Vision Res* **35**: 3083–3091.
33. Wong, AA and Brown, RE (2006). Visual detection, pattern discrimination and visual acuity in 14 strains of mice. *Genes Brain Behav* **5**: 389–403.
34. Brown, TM, Tsujimura, S, Allen, AE, Wynne, J, Bedford, R, Vickery, G *et al.* (2012). Melanopsin-based brightness discrimination in mice and humans. *Curr Biol* **22**: 1134–1141.
35. Dalkara, D and Sahel, JA (2014). Gene therapy for inherited retinal degenerations. *C R Biol* **337**: 185–192.
36. Morgan, JI, Hunter, JJ, Masella, B, Wolfe, R, Gray, DC, Merigan, WH *et al.* (2008). Light-induced retinal changes observed with high-resolution autofluorescence imaging of the retinal pigment epithelium. *Invest Ophthalmol Vis Sci* **49**: 3715–3729.
37. van Wyk, M, Pielecka-Fortuna, J, Löwel, S and Kleinlogel, S (2015). Restoring the ON Switch in Blind Retinas: Opto-mGluR6, a Next-Generation, Cell-Tailored Optogenetic Tool. *PLoS Biol* **13**: e1002143.
38. Burns, ME and Arshavsky, VY (2005). Beyond counting photons: trials and trends in vertebrate visual transduction. *Neuron* **48**: 387–401.
39. Masseck, OA, Spoida, K, Dalkara, D, Maejima, T, Rubelowski, JM, Wallhorn, L *et al.* (2014). Vertebrate cone opsins enable sustained and highly sensitive rapid control of Gi/o signaling in anxiety circuitry. *Neuron* **81**: 1263–1273.
40. Cao, P, Sun, W, Kramp, K, Zheng, M, Salom, D, Jastrzebska, B *et al.* (2012). Light-sensitive coupling of rhodopsin and melanopsin to G(i/o) and G(q) signal transduction in Caenorhabditis elegans. *FASEB J* **26**: 480–491.
41. Li, X, Gutierrez, DV, Hanson, MG, Han, J, Mark, MD, Chiel, H *et al.* (2005). Fast non-invasive activation and inhibition of neural and network activity by vertebrate rhodopsin and green algae channelrhodopsin. *Proc Natl Acad Sci USA* **102**: 17816–17821.
42. Grieger, JC, Choi, VW and Samulski, RJ (2006). Production and characterization of adeno-associated viral vectors. *Nat Protoc* **1**: 1412–1428.
43. Roska, B, Molnar, A and Werblin, FS (2006). Parallel processing in retinal ganglion cells: how integration of space-time patterns of excitation and inhibition form the spiking output. *J Neurophysiol* **95**: 3810–3822.